JACS
JOURNAL OF THE AMERICAN CHEMICAL SOCIETY

Article

pubs.acs.org/JACS

1,2-Dithiolane-Derived Dynamic, Covalent Materials: Cooperative Self-Assembly and Reversible Cross-Linking

Xiangyi Zhang and Robert M. Waymouth*

Department of Chemistry, Stanford University, Stanford, California 94305, United States

Supporting Information

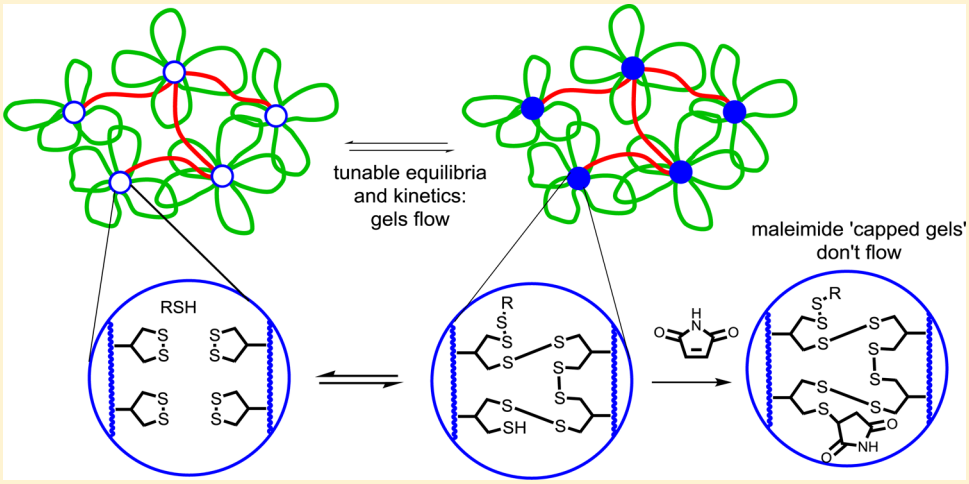

ABSTRACT: The use of dithiolane-containing polymers to construct responsive and dynamic networks is an attractive strategy in material design. Here, we provide a detailed mechanistic study on the self-assembly and gelation behavior of a class of ABA triblock copolymers containing a central poly(ethylene oxide) block and terminal polycarbonate blocks with pendant 1,2-dithiolane functionalities. In aqueous solution, these amphiphilic block copolymers self-assemble into bridged flower micelles at high concentrations. The addition of a thiol initiates the reversible ring-opening polymerizations of dithiolanes in the micellar cores to induce the cross-linking and gelation of the micellar network. The properties of the resulting hydrogels depend sensitively on the structures of 1,2-dithiolanes. While the methyl asparagusic acid-derived hydrogels are highly dynamic, adaptable, and self-healing, those derived from lipoic acid are rigid, resilient, and brittle. The thermodynamics and kinetics of ring-opening polymerization of the two dithiolanes were investigated to provide important insights on the dramatically different properties of the hydrogels derived from the two different dithiolanes. The incorporation of both dithiolane monomers into the block copolymers provides a facile way to tailor the properties of these hydrogels.

INTRODUCTION

New synthetic methods have revolutionized the synthesis of well-defined block copolymers.[1−5] The self-assembly of these macromolecules into complex supramolecular assemblies has created new opportunities for the generation of responsive and adaptive materials.[6−10] The self-assembly of block copolymers in solution is typically governed by thermodynamics of the noncovalent interactions that can be programmed into the block copolymer constituents.[11,12] Because of the reversible nature of noncovalent interactions, these materials exhibit complex dynamic behavior. Self-assembly can also be mediated by dynamic covalent interactions involving the reversible formation of covalent bonds.[13−15] Dynamic covalent materials constitute a class of adaptive complex materials.[14] The combination of noncovalent self-assembly and dynamic covalent chemistry leads to materials whose structural and dynamic properties are influenced by the kinetics and thermodynamics of both the supramolecular assemblies and the reversible bond formation.[14,16]

The emergent properties exhibited by dynamic covalent materials include self-healing[17−20] and shear-thinning behavior,[12,21] shape memory,[22] and the ability to respond to mechanical or chemical stimuli of their local environments.[14,23,24] Dynamic covalent hydrogels have found promising applications in tissue engineering;[25] their shear-thinning and viscoelastic properties also make them ideal injectable materials for cell delivery or 3D bioprinting.[7,26−28] Recent efforts have focused on materials incorporating orthogonal dynamic covalent chemistries to create complex and smart systems that can self-sort, adapt, amplify, replicate, transcribe,

Received: January 2, 2017
Published: February 28, 2017

ACS Publications © 2017 American Chemical Society

DOI: 10.1021/jacs.7b00039
J. Am. Chem. Soc. 2017, 139, 3822−3833

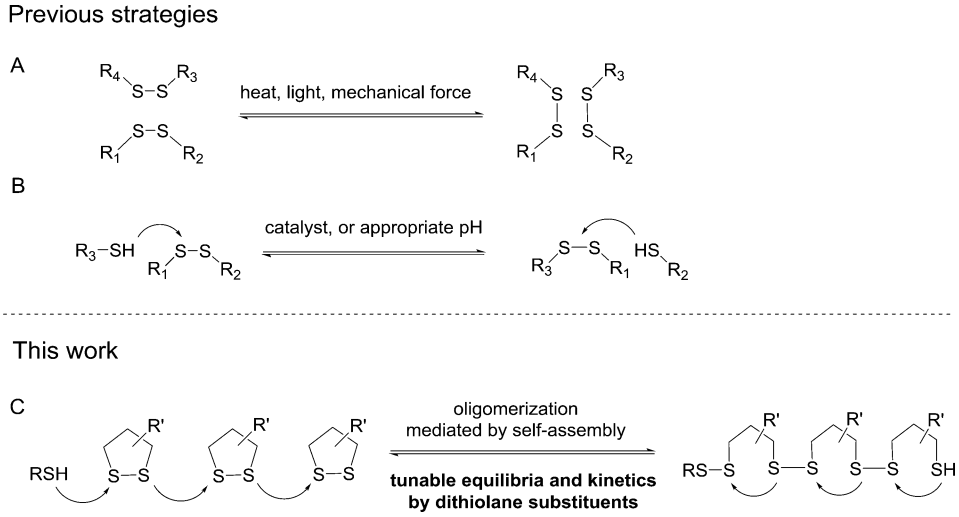

Figure 1. Dynamic covalent chemistry based on S−S bonds: (A) disulfide exchange, (B) thiol−disulfide exchange for linear disulfides, and (C) thiol-initiated ring-opening cascades of cyclic disulfides.

Scheme 1. Synthesis of Dithiolane-Functionalized Monomers and Block Copolymers

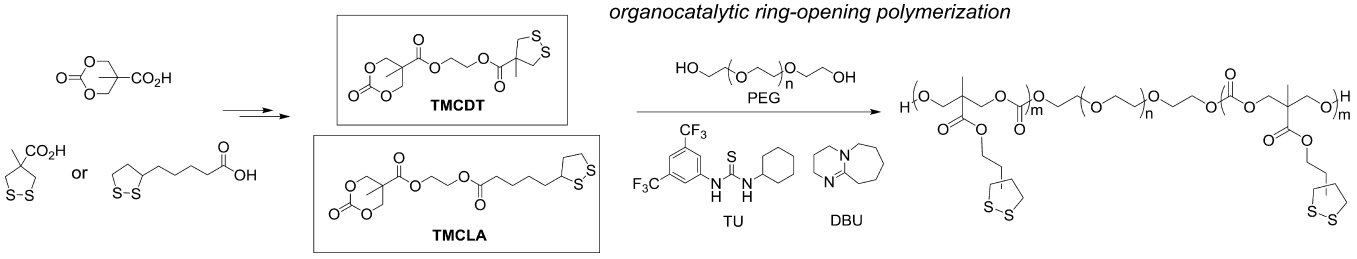

or exhibit complex adaptive behavior reminiscent of biological assemblies.[23,29]

Among the chemistries that have been employed for dynamic covalent chemistry, exchange reactions of disulfide bonds are particularly attractive as S−S bonds are strong, but undergo facile disulfide exchange reactions upon heating,[30,31] photo-irradiation,[32,33] or mechanical stress[34] (Figure 1A). The presence of endogenous or exogenous thiols can mediate reversible disulfide exchange reactions, depending on the pH (Figure 1B);[35,36] the dynamic exchange and shuffling of linear disulfides plays a crucial role in mediating the intracellular redox potential as well as protein folding and assembly. Reversible thiol−disulfide exchange has also been successfully applied to the design of self-healing and dynamic materials.[30−32,36−38]

In this report, we describe a strategy for reversibly cross-linking self-assembled supramolecular assemblies utilizing dynamic covalent chemistry that relies on the reversible cascade oligomerization of cyclic disulfides (Figure 1C)[39−41] facilitated by self-assembly. The use of cyclic 1,2-dithiolanes to cross-link and stabilize liposomes was shown by Regen;[42] related strategies have been used to generate redox-active nanoparticles and polymersomes.[43−51] Recently, Matile utilized the ring-opening polymerization of cyclic disulfides[39,40] to generate highly organized multicomponent architectures on solid surfaces.[52,53] They also synthesized a class of cell penetrating polydisulfides from dithiolanes substrates.[54,55] As shown by Whitesides,[56−59] an advantage of thiol/cyclic 1,2-dithiolane exchange reactions is that they are faster than reactions between thiols and linear disulfides and these reactions are both reversible and tunable, depending on the substituent pattern on the cyclic dithiolane ring. As described herein, this behavior provides a means of modulating the thermodynamic and kinetic stability of dynamic covalent materials utilizing dithiolanes as reversible cross-linkers.

In a previous report, we described a class of structurally dynamic hydrogels derived from 1,2-dithiolanes that were generated by organocatalytic polymerizations.[21] These materials were derived from water-soluble ABA triblock copolymers with hydrophilic poly(ethylene oxide) (PEG) B blocks and hydrophobic A blocks derived from carbonates bearing pendant 1,2-dithiolanes (Scheme 1). Upon the addition of a telechelic dithiol, these polymers form dynamic hydrogels that flow under applied stress and exhibit shear-thinning and self-healing behavior.[21] The dynamic properties of these hydrogels are easily modulated by pH, temperature, or the addition a thiol-capping agent such as maleimide, strongly indicating that the reversible thiol−disulfide exchange contributes to the dynamic properties of these hydrogels. In this report, we describe a comparative study on the structure and dynamic properties of hydrogels derived from ABA triblock copolymers bearing different pendant dithiolane groups. Through detailed mechanistic studies, we provide a comprehensive picture of the gelation mechanism that involves a cooperative self-assembly of triblock copolymers and reversible cross-linking based on thiol-initiated ring-opening cascade of dithiolanes. We also illustrate the large influence of dithiolane structure on the kinetics and thermodynamics of reversible cross-linking reactions that impact the physical and dynamic properties of these hydrogels.

DOI: 10.1021/jacs.7b00039
J. Am. Chem. Soc. 2017, 139, 3822−3833

Table 1. ABA Triblock Copolymers Containing Different 1,2-Dithiolanes[a]

copolymer	monomer	$[M]_0/[I]_0$	conv. %[b]	DP[c]	M_n[c] (kDa)	M_n[d] (kDa)	M_w/M_n[d]
1	TMCDT	10	87	8.5	16.9	12.4	1.16
2	TMCDT	12	86	9.8	17.4	13.2	1.15
3	TMCDT	14	87	11.7	18.1	14.0	1.18
4	TMCLA	8	90	7.2	16.8	11.7	1.13
5	TMCLA	10	88	8.8	17.4	12.8	1.14
6	TMCLA	12	89	10.7	18.2	13.6	1.14
7	TMCDT/TMCLA	6/4	87/89	5.2/3.6	17.2	12.7	1.17
8	TMCDT/TMCLA	4/6	86/90	3.5/5.8	17.5	13.0	1.18

[a]Polymerizations were performed in DCM at room temperature using 14 kDa PEG as the macroinitiator and $[M]_0 \approx 0.5$ M. [b]Conversion determined by ^{1}H NMR at 1.5 h. No further conversion was observed after extended reaction times. [c]Degree of polymerization (DP) of dithiolane-based monomers and number-average molar mass (M_n) determined by ^{1}H NMR. [d]Determined by GPC in THF with polystyrene calibration.

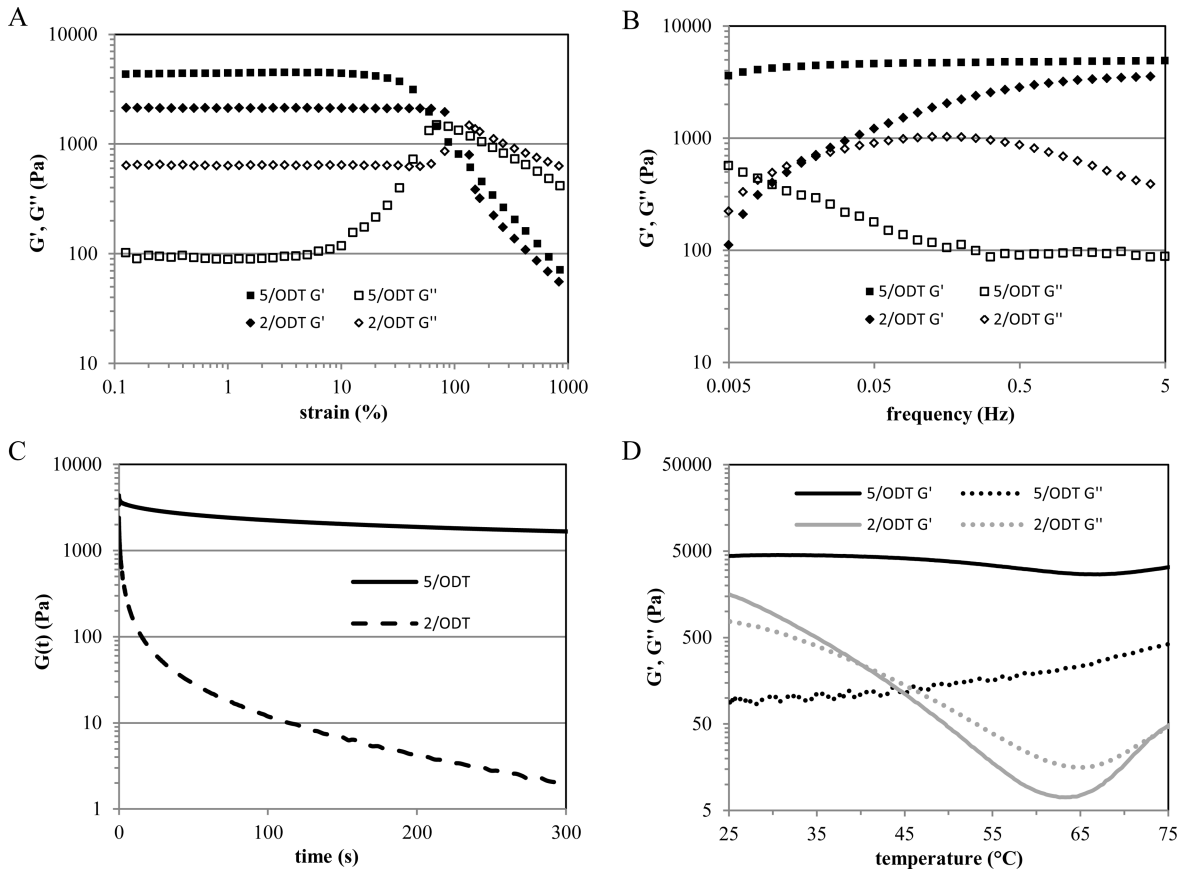

Figure 2. Rheological properties of hydrogels derived from copolymers **2** and **5** (10 wt % in water, cross-linked by 0.5 wt % ODT): (A) strain sweep at constant 1 Hz, (B) frequency sweep at constant 2% strain, (C) stress relaxation over time at 10% strain, and (D) temperature ramp at constant 1 Hz and 2% strain.

RESULTS AND DISCUSSION

Synthesis of Dithiolane-Functionalized Triblock Copolymers. Two 1,2-dithiolane-functionalized cyclic carbonate monomers (TMCDT and TMCLA) were synthesized in two steps from methyl asparagusic acid or lipoic acid (Scheme 1). The two monomers exhibited different stabilities at room temperature: while TMCDT was a stable crystalline solid, TMCLA was a heavy oil that readily autopolymerized upon concentration and needed to be stored as a dilute solution. This observation implies different reactivities of the two dithiolanes toward ring-opening. Subsequent ring-opening polymerizations of TMCDT and TMCLA were performed in dichloromethane at room temperature using a 14k PEG initiator and 5 mol % thiourea and DBU catalyst. At an initial monomer concentration $[M]_0$ = 1.0 mol/L, the polymerization of TMCDT proceeded rapidly and generated well-defined triblock copolymers **1**−**3** with narrow molecular weight distributions (M_w/M_n < 1.2). In contrast, the reaction mixture of TMCLA gelled as soon as the polymerization started, suggesting a concurrent ring-opening of cyclic carbonates and dithiolanes. When $[M]_0$ was lowered to 0.5 mol/L, the polymerization of TMCLA proceeded cleanly to high conversion (~88%) to afford the desired triblock copolymers **4**−**6** with intact dithiolanes, as revealed by ^{1}H NMR (Supporting Information, NMR spectra). These observations provide further evidence that the ring-opening of the cyclic disulfides of TMCLA occurs more readily than that of TMCDT, especially at high concentration. The

DOI: 10.1021/jacs.7b00039
J. Am. Chem. Soc. 2017, 139, 3822−3833

block lengths of these triblock copolymers can be precisely controlled by the monomer to PEG initiator ratios (Table 1).

Copolymerization of TMCDT and TMCLA under the same catalytic condition provides triblock copolymers **7** and **8** that contain a mixture of lipoic acid and methyl asparagusic acid-derived dithiolanes appended to the chains. The relative ratios of the two dithiolanes incorporated in the polymers were determined by ^{1}H NMR analysis (Supporting Information, NMR spectra). Copolymer **7** has a higher TMCDT content with a ratio of TMCDT/TMCLA = 1.44, while copolymer **8** contains more TMCLA units with a ratio of TMCDT/TMCLA = 0.60 (Table 1). The relative contents of the two dithiolane groups in the copolymers can be easily tuned by comonomer feed ratios.

Preparation and Properties of Thiol-Cross-Linked Hydrogels. The triblock copolymers with a 14 kDa hydrophilic PEG block and two short hydrophobic end blocks can be readily dissolved in water at 10 wt %. Addition of a dithiol such as 3,6-dioxa-1,8-octanedithiol (ODT, 0.5 equiv relative to dithiolanes) to the aqueous dispersions of copolymers **1**−**8** results in rapid gelation. Previous studies[21] showed that the hydrogels derived from TMCDT-derived copolymers **1**−**3** are structurally dynamic networks that are adaptable, flow under applied stress, and rapidly self-heal after deformation. The dynamic behavior of these materials depends on the architecture (block length) of the polymers and can be easily modulated by environmental factors such as pH, temperature, and the presence of a thiol capping agent such as maleimide.[21]

Despite the similar architecture and composition of copolymers **1**−**3** (derived from TMCDT) and **4**−**6** (derived from TMCLA), the hydrogels derived from the lipoic acid-functionalized monomer TMCLA showed dramatically different properties from the TMCDT-derived hydrogels. Unlike the TMCDT-derived gels, which are deformable and moldable, TMCLA-derived gels are rigid and maintain their shapes once formed. TMCDT-derived gels flow over the course of hours in a vial inversion test, whereas no creep was observed for TMCLA gels on the same time scale. Moreover, TMCLA gels showed poor self-healing capability. Hydrogels derived from TMCLA fractured easily under applied force and were unable to repair the damage. These surprisingly large differences between TMCDT and TMCLA gels indicated that the structure and substituent pattern of dithiolanes have a significant impact on the macroscopic properties of these materials.

To characterize the dynamic properties of these materials, small amplitude oscillatory shear rheometry measurements were carried out on two different hydrogels derived from copolymers **2** and **5** (Table 1). First, a strain sweep was performed at constant frequency (1 Hz) to investigate the response of gels to strains with different amplitudes. As shown in Figure 2A, the TMCDT-derived hydrogel **2**/ODT exhibited a linear viscoelastic response with a constant G' = 2130 Pa and G'' = 640 Pa up to 90% strain, whereas the TMCLA-derived hydrogel **5**/ODT exhibited a linear viscoelastic behavior from 0.1% to only 5% strain with a higher storage modulus G' = 4400 Pa and lower loss modulus of G'' = 90 Pa. The higher G' and lower G'' of the gel derived from the **5**/ODT gel is consonant with visual observations that TMCLA gels are more rigid and less fluid than TMCDT gels. The narrow linear viscoelastic region of **5**/ODT indicated that it cannot withstand as much strain as the TMCDT gel before it is structurally disrupted. Both gels exhibited network failure at large strains with a sharp decrease in G' and a crossover of G' and G'' at ∼200% strain for **2**/ODT and ∼60% strain for **5**/ODT, indicative of significant disruption of the network structure.

Repetitive step-strain measurements performed at high (γ = 200%) and low (γ = 1%) strains at a constant frequency (1 Hz, Figure S1) revealed that the TMCLA-derived hydrogel **5**/ODT exhibited poor recovery after a large step-strain and the moduli G' and G'' did not return to their original values when the large strain was removed. The gel fractured and was expelled from the rheometer at the end of measurement, indicative of a poor self-healing behavior. In contrast, the gels derived from TMCDT-based **2**/ODT exhibited exceptionally fast and complete recovery of its mechanical strength after several cycles of large deformations.[21]

The frequency dependence of the storage and loss shear moduli (G' and G'') is shown in Figure 2B. The gel derived from **2**/ODT exhibits the typical viscoelastic behavior of transient networks[24] as the storage modulus G' is higher than the loss modulus G'' at high frequencies but decreases below G'' at lower frequencies. In contrast, for the gel derived from **5**/ODT, G' is nearly independent of frequency and is higher than G'' across the entire frequency range (0.005−5 Hz), characteristic of an elastic material. This difference is consistent with observations that TMCLA gel does not flow under applied stress even on a long time scale.

The stress relaxation behavior of the gels was explored to compare their ability to store or dissipate energy. Following an initial 10% strain, the stress response $G(t)$ was recorded over time. The TMCDT-derived hydrogel **2**/ODT relaxed 90% of the stress within a few seconds, while the TMCLA-derived hydrogel **5**/ODT relaxed only ∼50% stress after 5 min (Figure 2C). These stress relaxation curves are not readily fit to the Maxwell−Weichert model,[60] suggesting that these hydrogels have a complex stress relaxation mechanism involving multiple relaxation modes that might be dependent on one another. Nevertheless, if we define a relaxation time τ as the time it takes the materials to relax to $1/e$ of their original stress, then τ = 1 s for the gel derived from **2**/ODT, whereas τ = 420 s for the gel derived from **5**/ODT. These results reveal that TMCDT gels can dissipate an applied force at a much higher rate than TMCLA gels.

The temperature dependence of the moduli was examined by a temperature ramp from 25 to 85 °C at a heating rate of 2 °C/min (Figure 2D). As demonstrated previously,[21] the TMCDT-derived hydrogel **2**/ODT is thermoresponsive and exhibits a reversible sol−gel transition at 42 °C. When the temperature increased above 65 °C, the solution became cloudy and both G' and G'' increased. At approximately 80 °C, the polymer precipitated out of the solution. This phase separation is caused by the dehydration of PEG approaching its LCST (85−100 °C) and is commonly observed for PEG-based amphiphilic block copolymers.[61,62] In contrast, the TMCLA gels show a moderate increase in G'' and almost constant G' between 25 and 75 °C with no evident sol−gel transition over this temperature range, demonstrating a higher thermal stability.

Another notable difference between the two gels is their stability against dilution. A disk of **2**/ODT or **5**/ODT gel (100 μL) formed in a 1/2 dram vial was removed from the vial and placed in a 200 mL water bath. The TMCDT-derived hydrogel **2**/ODT lost 50% of its original mass in the first hour and completely dissolved in 3 h (Figure S3), whereas the TMCLA-derived hydrogel **5**/ODT swelled in water with a significant increase in mass (∼50%) that persisted for a period of 24 h.

DOI: 10.1021/jacs.7b00039
J. Am. Chem. Soc. 2017, 139, 3822−3833

Taken together, these remarkable differences between the two structurally similar hydrogels highlight the importance of dithiolane structure on the rheological properties and network stabilities of these dithiol-cross-linked gels.

With two remarkably different hydrogels in hand, we sought to prepare hydrogels with intermediate properties by incorporating both dithiolanes into the polymer chains. The rheological properties of hydrogels prepared from copolymers **7** and **8** (Table 1) that contain a mixture of TMCDT and TMCLA were investigated (Figure S2). As compared to the gels derived from **2**/ODT and **5**/ODT, the hydrogels derived from **7**/ODT and **8**/ODT exhibited intermediate G' and G'' and stress relaxation rates (τ = 3 s for **7**/ODT and τ = 40 s for **8**/ODT). Both gels exhibited better recovery of G' and G'' than gels derived from **5**/ODT following a large amplitude strain. While gels derived from **7**/ODT (with an excess of TMCDT) are viscoelastic with a $G'-G''$ crossover frequency of 0.007 Hz, the gels derived from **8**/ODT (with an excess of TMCLA) are predominantly elastic with $G' > G''$ at all measured frequencies. The dissolution rates of these gels in water were slower than those derived from **2**/ODT but faster than those derived from **5**/ODT (Figure S3). These results clearly showed that the properties of the hydrogels can be modulated by controlling the type and ratio of both monomers incorporated into the structure. Their rheological properties depend on the relative content of the two dithiolanes: gels derived from **7**/ODT with a TMCDT/TMCLA = 1.44 exhibits properties closer to TMCDT gels, while those derived from **8**/ODT with a TMCDT/TMCLA = 0.60 are more comparable to TMCLA gels. Therefore, the moduli, stress relaxation rates, and viscoelastic properties of these comonomer-derived hydrogels can be systematically varied by simply adjusting the comonomer feed ratios. This provides a facile route to tailor the properties of the gels for different applications.

Gelation Mechanism. In our previous report,[21] we had suggested that the dynamic properties of these dithiolane-derived hydrogels might be due to a combination of self-assembly of hydrophobically associated TMCDT blocks and thiol−disulfide exchange. To assess the role of self-assembly and disulfide exchange, we carried out a series of experiments to investigate these factors independently. It is well established that amphiphilic ABA triblock copolymers containing hydrophilic central blocks and hydrophobic terminal blocks self-assemble in water to form flower micelles, which at higher concentrations form physical gels that behave as transient networks (Figure 3).[7,9,10,12,63]

To assess the role of self-assembly on the properties of these materials, we investigated the self-assembly of the triblock copolymers **2** and **5** at different concentrations in water. The formation of micelles from triblock copolymers **2** and **5** in dilute solution was characterized by the fluorescence spectroscopy of pyrene, a solvatochromic probe that exhibits different emission profiles when it transitions from a hydrophilic (water) to hydrophobic (core of the micelles) environment.[64] The onset of the transition was used as a measure of the critical micelle concentration (CMC). The CMC of copolymer **2** was determined to be 0.354 mg/mL, and that of **5** was 0.310 mg/mL (Figure 5 and Figure S4). The micelles of copolymers **2** and **5** were characterized by dynamic light scattering (DLS) measurements. At a concentration slightly above CMC (0.5 mg/mL), micelles derived from copolymer **2** showed a single distribution with a *z*-average hydrodynamic diameter (D_H) of 28 nm, whereas those from copolymer **5** had a D_H = 37 nm (Figure 4, solid lines). These data are consistent with the formation of flower micelles where the terminal dithiolane-containing blocks associate through hydrophobic interactions with a corona of swollen PEG chains. The average number of polymer chains residing in individual micelles (aggregation number N_{agg}) was determined by static light scattering measurements performed at concentrations slightly above CMC[65] (Figure S5) and revealed that N_{agg} = 7.5 for copolymer **2** and N_{agg} = 8.5 for copolymer **5** (Figure 5).

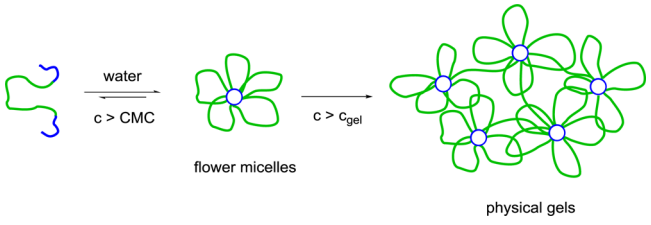

Figure 3. Self-assembly and gelation of amphiphilic ABA triblock copolymers.[7,9,10,12,63]

At a higher concentration (5 mg/mL), a second distribution with a much larger size appeared at 165 nm for copolymer **2** (Figure 4A). This is attributed to the formation of micellar clusters through the rearrangement of the looping chains (A block) to bridging chains that serves to connect adjacent micelles (Figure 3).[8] As the concentration was increased further (20 mg/mL), the relative intensity of the second peak increased, and the size of these micellar clusters increased to 220 nm, indicating more micelles participated in the formation of larger clusters. Similar behavior was observed for copolymer **5** where flower micelles with D_H = 37 nm were observed at concentrations of 0.5 mg/mL, but aggregated at higher concentrations (Figure 4B).

The rheological properties of these uncross-linked polymers in water were investigated at higher concentrations; these experiments revealed that at 100 mg/mL (10 wt %, a concentration comparable to that of the cross-linked gels, Figure 2), aqueous solutions of copolymers **2** and **5** are viscous liquids rather than gels, exhibiting loss moduli G'' (**2**, 43 Pa; **5**, 84 Pa) that are greater than the storage moduli G' (**2**, 23 Pa; **5**, 66 Pa, Figure S6). These data suggest that at concentrations of 10 wt %, the uncross-linked copolymers **2** and **5** are just below the critical gel concentration where the number of ABA chains spanning different micelles is insufficient to form robust physical gels.[12,63]

At higher concentrations (15 wt %), both copolymers **2** and **5** form physical gels with the storage moduli G' higher than the loss moduli G'' and a broad linear viscoelastic region (0.1−100% strain, Figure S6). At higher applied strains (>100%), both G' and G'' drop, and G' decreases below G'' at ∼165% strain as a consequence of shear-induced disruption of physical cross-links (intermicellar bridges, Figure 3).[12] The physical gels of copolymers **2** and **5** exhibited comparable viscoelastic behavior with a crossover of G' and G'' at ∼0.06 and ∼0.03 Hz for copolymers **2** and **5**, respectively (Figure S7a). Both gels could quickly relax applied stress (τ = 0.6 s for copolymer **2** and 0.8 s for copolymer **5**) (Figure S7b). A dynamic step-strain test showed that these physical gels had relatively slow recovery: after the large strain (800%) was removed, the gels did not fully recover their initial G' in the given amount of time (1 min) but returned to a lower G' (Figure S7c,d), indicating that the time scale for reforming the physical cross-links and re-equilibrating

DOI: 10.1021/jacs.7b00039
J. Am. Chem. Soc. 2017, 139, 3822−3833

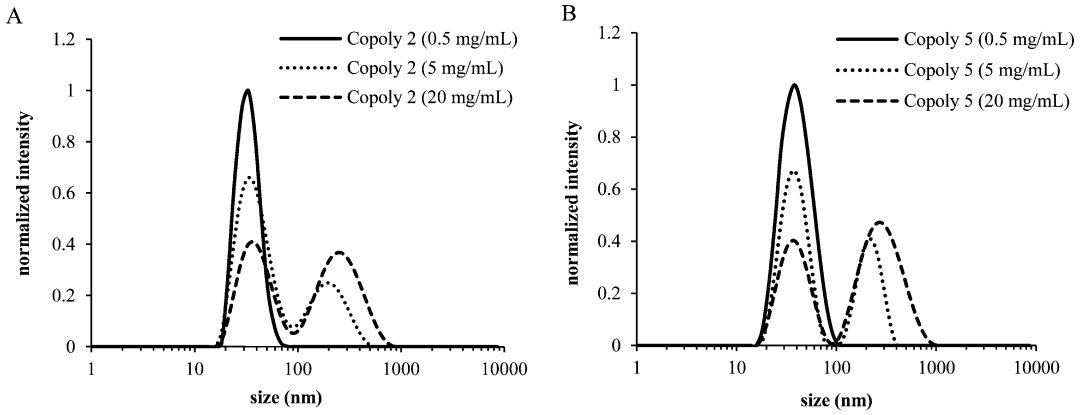

Figure 4. Size distribution determined by DLS for copolymers **2** (A) and **5** (B) in water as a function of concentration. The intensity distribution was normalized and plotted against size in nanometers. The size of the micelles shows a concentration-dependent profile.

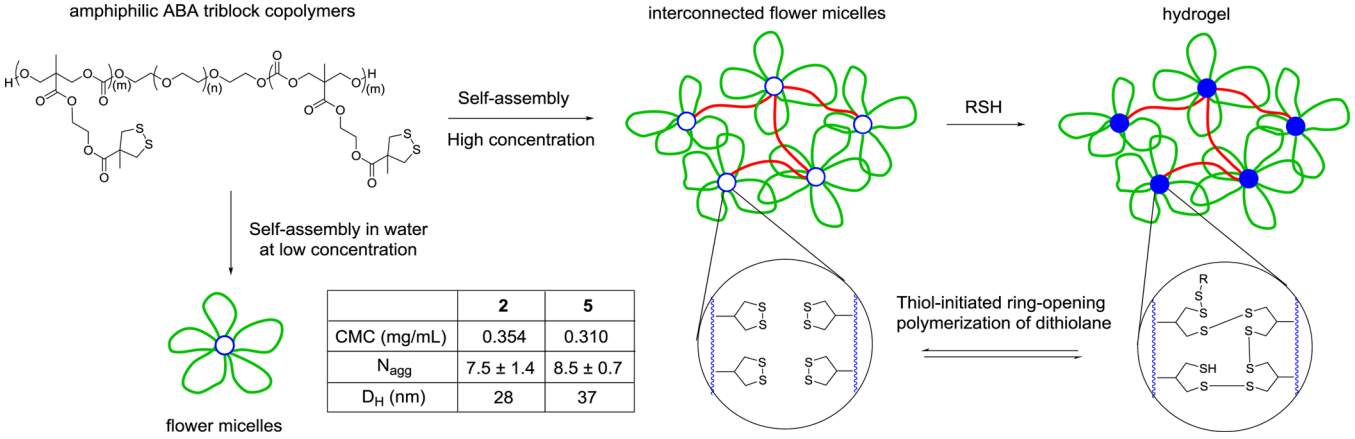

	2	5
CMC (mg/mL)	0.354	0.310
N_{agg}	7.5 ± 1.4	8.5 ± 0.7
D_H (nm)	28	37

Figure 5. Proposed gelation mechanism for dithiolane-containing triblock copolymers in the presence of thiols. The physical cross-linking via the bridging PEG chains was shown in red. The chemical cross-linking via the thiol-initiated ring-opening polymerization of dithiolanes was shown in blue.

is slow.[66] Taken together, these studies reveal that triblock copolymers **2** and **5** self-assemble in water and form physical gels at concentrations ≥15 wt %, but the resulting gels exhibit much lower moduli than the cross-linked gels (Figure 2), and, in contrast to the cross-linked gels, the physical gels derived from copolymers **2** and **5** exhibit qualitatively similar behavior. This behavior is different from the cross-linked gels formed with the dithiol ODT at 10 wt %, indicating that the properties of the physical gels are not very sensitive to the nature of the pendant dithiolane (TMCDT or TMCLA).

Role of Thiol−Disulfide Exchange on Dynamic Cross-Linking. In addition to the self-assembly of these triblock copolymers, the mechanism of the chemical gelation induced by a thiol cross-linker was closely examined. In our previous study,[21] we proposed that telechelic dithiols can undergo thiol−disulfide exchange with two pendant dithiolanes from different polymer chains to facilitate cross-linking. The following experiments indicate that this hypothesis was incorrect. To assess the role of disulfide cross-linking independent of self-assembly, we attempted to cross-link the block copolymers **1**−**8** with the dithiol ODT in organic solvents. Addition of ODT to an organic solution of copolymers **1**−**8** (10 wt % in dichloromethane or acetone) did not result in gelation. Moreover, no gelation was observed for a random copolymer of TMCDT and a PEGylated carbonate monomer, which have compositions similar to those of copolymers **1**−**3** (Supporting Information, p S5). These observations imply that the self-assembly of these block copolymers in water is a necessary condition for thiol-mediated cross-linking to occur (Figure 5).

Additional insight on the cross-linking mechanism was obtained by the demonstration that thiols such as mercaptoethanol are as effective as telechelic dithiols at inducing the gelation of these triblock copolymers in water. At a concentration of 10 wt % of copolymer **2**, even a substoichiometric amount of a monothiol (0.1 equiv of 2-mercaptoethanol relative to dithiolanes) is able to trigger the gelation of a 10 wt % solution of copolymer **2**. Moreover, the hydrogels prepared from a monothiol or a dithiol cross-linker show similar rheological properties as long as the total concentration of thiol is the same (Figure S8). These results suggest that the cross-linking occurs through a thiol-initiated ring-opening polymerization of dithiolanes[39,52,67] (Figure 1c, Figure 5), in which each thiol−disulfide exchange forms a thiol that can propagate with another dithiolane.

The mechanism proposed in Figure 5 would suggest that the self-assembly of the hydrophobic dithiolanes at the core of the micelles is critical to enable a monothiol to be effective as a cross-linker. To further test this proposed mechanism and assess its implications, we investigated the thiol-initiated cross-linking chemistry on the self-assembled micelles (Figure 6). A substoichiometric amount of 2-mercaptoethanol (relative to dithiolanes) was introduced to a dilute solution (1.5 mg/mL)

DOI: 10.1021/jacs.7b00039
J. Am. Chem. Soc. 2017, 139, 3822−3833

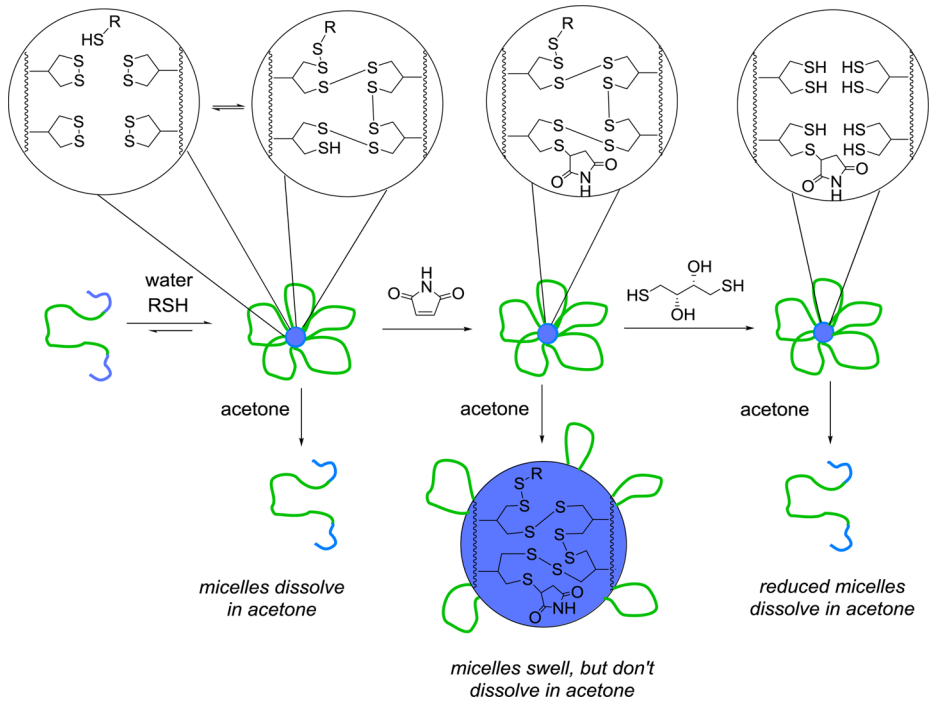

Figure 6. Demonstration of the thiol-initiated cross-linking chemistry in the context of micelles. Flower micelles formed through the self-assembly of copolymers **2** and **5** dissociated upon the addition of acetone; micelles cross-linked by a thiol also dissociated in acetone; micelles cross-linked by a thiol and capped with maleimide persisted in acetone; micelles cross-linked by a thiol, capped with maleimide, and then treated with dithiothreitol dissociated in acetone.

of copolymers **2** and **5**, a concentration above the critical micelle concentration (CMC) but below that of gelation. The ring-opening of dithiolanes was followed by UV−vis spectroscopy (Figure S9). The characteristic absorbance of dithiolane functionality at ∼330 nm decreased upon the addition of thiol but did not fully disappear, indicating a significant but not complete ring-opening of dithiolanes. When these cross-linked micelles were dispersed in acetone, a good solvent for both the PEG and polycarbonate blocks, they completely dissolved to free polymer chains as no particles were detected by DLS measurements (Figure 6). In contrast, when we treated the micelles first with mercaptoethanol and then with maleimide, these micelles persisted upon the addition of acetone and showed a moderate increase in size (Figure S10). These results provide evidence that the core of the micelles can be cross-linked through thiol−disulfide ring-opening cascade of dithiolanes; yet, this cross-linking is reversible, and upon dilution, the reversible depolymerization of the polydisulfide in the core regenerates the uncross-linked dithiolane rings, resulting in dissolution of the micelles. However, if the terminus of the polymerized diothiolanes is capped by the addition of maleimide,[21,67] the depolymerization of the polysulfide is inhibited, preventing the micelles from dissociation upon the addition of acetone.

We further showed that these core-cross-linked micelles can be readily disintegrated under reducing conditions. Upon treatment of the thiol-cross-linked micelles (end-capped by maleimide) with 10 mM dithiothreitol (DTT), the micelles completely dissolved upon the addition of acetone, as no particles could be detected by dynamic light scattering (Figure 6). These redox-sensitive core cross-linked micelles could comprise a potentially useful delivery platform for therapeutics.[43,46,48,50,68−70]

These mechanistic studies provide compelling support for a gelation mechanism (Figure 5), which involves a combination of physical cross-linking induced by self-assembly and aggregation of flower micelles and chemical cross-linking induced by thiol-mediated ring-opening polymerization of dithiolanes concentrated in the hydrophobic core of the micelles. In aqueous solution, the hydrophobic interaction between the dithiolane blocks drives the self-assembly of the triblock copolymers to form flower micelles. As concentration increases, micelles are closer to each other and entropy favors the reorganization of PEG chains from a loop conformation to an extended conformation where the two hydrophobic ends reside in different micelles. This leads to a physical cross-link between micelles. The addition of thiols triggers the dynamic cross-linking of micellar cores through a rapid and reversible ring-opening cascade of dithiolanes. The resulting hydrogel is a micellar network physically cross-linked through the hydrophilic PEG chains and chemically cross-linked via disulfide bonds.

Ring-Opening Polymerization of Dithiolanes. Because the self-assembly behaviors of copolymers **2** and **5** are similar as are the properties of their physical gels, the remarkably different properties between the thiol-cross-linked hydrogels **2**/ODT and **5**/ODT likely arise from the different kinetics and thermodynamics of thiol-initiated cross-linking of dithiolanes.

Whitesides' early studies on thiol−disulfide exchange reactions of thiols with cyclic disulfides indicated that both ring size and substituent pattern have a significant impact on the equilibria and rates of thiol-induced ring-opening of cyclic disulfides.[56−59] Nevertheless, despite intense interest in the mechanism of thiol-disulfide exchange for both linear[71,72] and cyclic disulfides,[41,54,56−58,73] many aspects of the thermodynamics and kinetics of the ring-opening of dithiolanes remain poorly understood. We show here that the organocatalytic

DOI: 10.1021/jacs.7b00039
J. Am. Chem. Soc. 2017, 139, 3822−3833

Scheme 2. Synthesis of Dithiolane Monomers and Ring-Opening Polymerizations of Dithiolanes

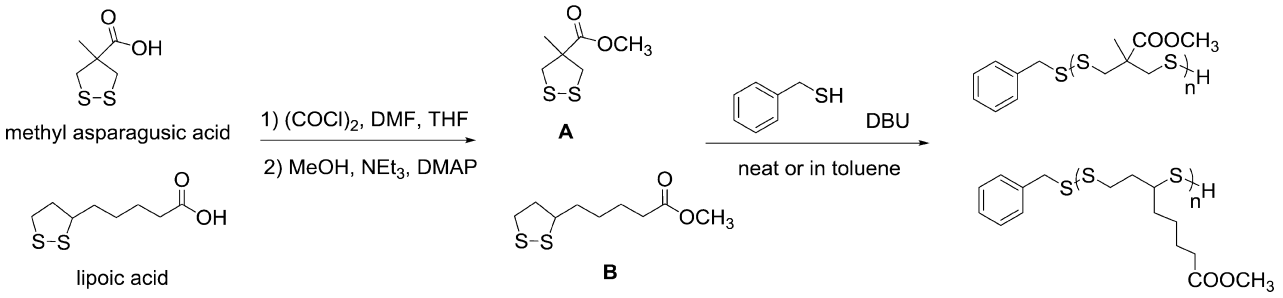

Table 2. Thermodynamic and Kinetic Data for Ring-Opening Polymerization of 1,2-Dithiolanes

Monomer	$[M]_{eq}$, 23 °C [a] M	K_{eq}, 23 °C [b] M^{-1}	ΔH_p [c] kJ/mol	ΔS_p [c] J/(mol·K)	k_{obs} [d] min^{-1}
A 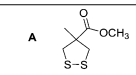	2.95	0.339	-9.99	-43.35	1.384
B 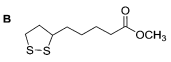	0.93	1.075	-15.44	-50.84	0.308

[a]Equilibrium monomer concentration determined as the final monomer concentration in equilibrated reactions. [b]Equilibrium constant of the polymerization−depolymerization equilibrium determined by $1/[M]_{eq}$. [c]Standard enthalpy and entropy of the propagation determined from the slope and intercept of the van't Hoff plots. [d]Observed rate constants obtained from the kinetics of the polymerization.

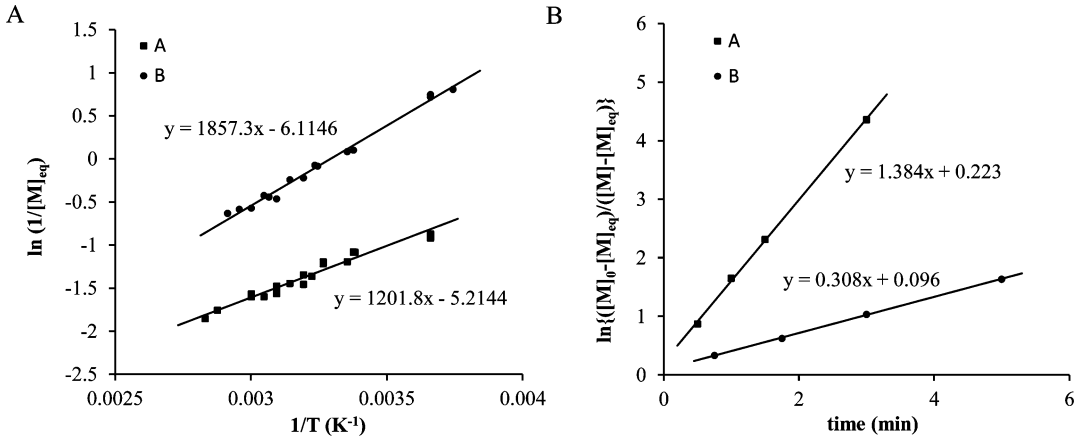

Figure 7. (A) Temperature dependence of equilibrium monomer concentration of ring-opening polymerization of **A** and **B**. (B) First-order kinetics of ring-opening polymerizations of **A** and **B**.

polymerization[39,41] of dithiolanes can provide useful thermodynamic and kinetic data on the role of substituents on dithiolane ring-opening equilibria. These data provide both useful insights on the origin of the different macroscopic behaviors of the different hydrogels, as well as fundamental insights on the thermodynamics and kinetics of thiol−disulfide exchange reactions.

We prepared two model monomers **A** and **B** from the corresponding methyl asparagusic acid and lipoic acid via acyl chloride intermediates (Scheme 2, Supporting Information, p 8). Ring-opening polymerizations of **A** and **B** were carried out in toluene under N_2 using benzyl mercaptan as an initiator and DBU as a catalyst. These polymerizations occurred readily at room temperature but stopped at moderate conversions even at high initial monomer concentrations (Table S1). No further monomer conversions were observed when the concentration of monomer approached 2.95 M for **A** and 0.93 M for **B** regardless of the initial monomer and initiator concentrations, indicative of an approach to thermodynamic equilibrium. To verify that the limited conversions of these polymerizations are a consequence of polymerization−depolymerization equilibria instead of chain termination events, we carried out a depolymerization experiment in which a polymerization performed at high initial monomer concentrations was diluted by toluene. ^{1}H NMR analysis of the reaction mixture revealed that depolymerization occurred after dilution and a new equilibrium was achieved with a final monomer concentration $[M]_f$ = 2.95 M. Upon further dilution, the polymer fully depolymerized back to monomer (Supporting Information, p S10, Figure S12). In a control experiment, excess benzoic acid or maleimide was introduced to the reactions before dilution, and no depolymerization occurred. These results indicate that the polymerization is completely reversible and the conversion is dictated by thermodynamic equilibria. Therefore, the equilibrium monomer concentrations of these polymerizations can be correlated to the final monomer concentrations in the ring-opening polymerization reactions, yielding the following

DOI: 10.1021/jacs.7b00039
J. Am. Chem. Soc. 2017, 139, 3822−3833

estimates for the equilibrium monomer concentrations: $[M]_{eq}$ = 2.95 M for **A** and $[M]_{eq}$ = 0.93 M for **B** at 23 °C (Table 2). ^{1}H NMR spectra of the resulting polydisulfides revealed a benzyl mercaptan end group (Figure S11). The molecular weights based on the end group analysis were close to those obtained from GPC analysis and roughly correlated with those predicted from $[M]_0/[I]_0$ and conversions (Table S1). The molecular weight distributions of these polymers are close to 2.0, which is the most probable distribution of thermodynamic equilibrated polymerizations.[74,75]

For polymerization−depolymerization equilibria (eq 1), the equilibrium constant K_{eq} is related to $[M]_{eq}$ by eq 2, assuming $[P_n^*] = [P_{n+1}^*]$.[74,75] According to eq 2, K_{eq} for monomer **A** and **B** is 0.339 and 1.075 M^{-1}, respectively, at 23 °C. Therefore, the equilibrium constant of chain propagation for **B** is 3.2 times higher than that for **A**.

$$P_n^* + M \underset{k_d}{\overset{k_p}{\rightleftharpoons}} P_{n+1}^* \tag{1}$$

$$K_{eq} = \frac{[P_{n+1}^*]}{[P_n^*][M]_{eq}} = 1/[M]_{eq} \tag{2}$$

$$\ln\left(\frac{1}{[M]_{eq}}\right) = \frac{-\Delta H_p^0}{RT} + \frac{\Delta S_p^0}{R} \tag{3}$$

The temperature dependence of K_{eq} (eq 3) was used to determine the enthalpy and entropy of ring-opening polymerization through the slope and intercept of the van't Hoff plots shown in Figure 7A. The thermodynamic parameters obtained were ΔH_p^0(**A**) = −9.99 kJ/mol, ΔS_p^0(**A**) = −43.35 J/(mol·K) for **A** and ΔH_p^0(**B**) = −15.44 kJ/mol, ΔS_p^0(B) = −50.84 J/(mol·K) for **B** (Table 2). Therefore, the ring-opening polymerization of dithiolanes is driven by the enthalpy of ring-opening as a result of release of ring strain. Dithiolane **B** has a ΔH_p^0 that is 5.45 kJ/mol more negative than that of dithiolane **A**, indicating a larger ring strain of lipoic acid relative to that of methyl asparagusic acid.

The kinetics of these ring-opening polymerizations of dithiolanes were investigated by monitoring the evolution of the monomer conversion as a function of time. The concentration of benzyl mercaptan and DBU was $[BnSH]_0$ = 0.01 M and [DBU] = 0.005 M throughout all measurements. For a reversible polymerization with a propagation rate constant k_p and a depropagation rate constant k_d, the overall monomer consumption rate is expressed in eq 4.[74] Integration of eq 4 leads to the expression of monomer concentration as a function of time (eq 5):

$$R_p = -\frac{d[M]}{dt} = k_p \sum [P_n^*][M] - k_d \sum [P_{n+1}^*] \tag{4}$$

$$\ln \frac{[M]_0 - [M]_{eq}}{[M] - [M]_{eq}} = k_p \sum [P_n^*]t = k_p[I]_0 t \tag{5}$$

Plots of $\ln[([M]_0 - [M]_{eq})/([M] - [M]_{eq})]$ versus time for the ROP of **A** and **B** are shown in Figure 7B. The linearity of the curve is indicative of first-order kinetics for the disappearance of monomer. The observed rate constant (k_{obs}) obtained from the slope of the linear fit is 1.384 min^{-1} for **A** and 0.308 min^{-1} for **B** (Table 2). Given that the concentration of initiator and catalyst was the same for the polymerizations of **A** and **B**, the ratio of k_{obs}(**A**) to k_{obs}(**B**) yields a good estimate of k_p(**A**)/k_p(**B**). Therefore, the propagation rate of monomer **A** is ∼4.5 times faster than that of **B**. On the basis of the fact that $K_{eq} = k_p/k_d$ for the polymerization−depolymerization equilibrium (eq 1), the depropagation rate constant k_d for dithiolane **A** is approximately 14 times faster than that for **B**.

The kinetic and thermodynamic data can be used to estimate the energy profile of the chain propagation step as shown in Figure 8. The chain propagation equilibrium of the methyl asparagusic acid monomer **A** has a K_{eq} < 1 and therefore a positive standard free energy change ($\Delta G_p^0 \approx$ 2.7 kJ/mol, 23 °C) for the propagation. In contrast, methyl lipoate **B** has a K_{eq} > 1 and a negative standard free energy change ($\Delta G_p^0 \approx -0.2$ kJ/mol, 23 °C). The energy barrier for both the propagation and the depropagation reaction of **A** is lower than that for **B**, and thus the rate of ring-opening and closure of dithiolane **A** is faster than that of **B**. The difference in activation energy ($\Delta G^{\ddagger}_A - \Delta G^{\ddagger}_B$) is more significant for the depropagation than the propagation step. While the propagation rate constant for **A** is approximately 4.5 times higher than that for **B**, the depropagation rate constant is 14 times higher than for **B**.

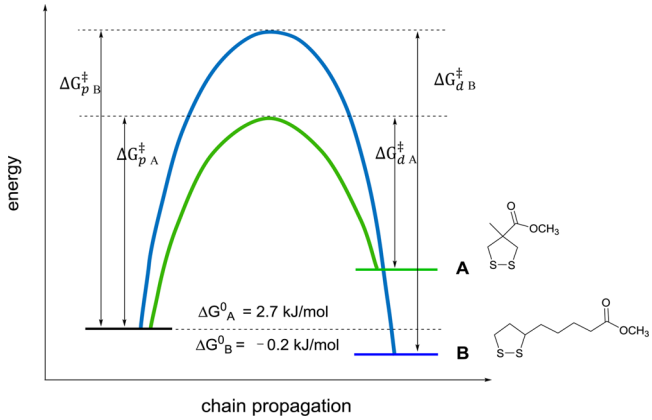

Figure 8. Energy profile of the propagation and depropagation equilibria for the ring-opening polymerization of dithiolane **A** and **B**.

Role of Kinetics and Thermodynamics on the Physical and Dynamic Properties of Dithiolane Hydrogels. The thermodynamic and kinetic data of the ring-opening polymerizations of dithiolanes provide insights on the influence of the different dithiolanes on the macroscopic properties of corresponding hydrogels. The ring-opening polymerizations of methyl asparagusic acid derivatives, which have lower ring strains, are thermodynamically less favorable than those of the lipoic acid derivatives. Nevertheless, the kinetic barriers for both the ring-opening and the ring-closing of methyl asparagusic acid derivatives are much lower, resulting in a faster cross-linking and de-cross-linking of the network and therefore the formation of a more dynamic and labile network.

The high $[M]_{eq}$ of these ring-opening polymerizations of dithiolanes requires a high initial dithiolane concentration ($[M]_0 > [M]_{eq}$) for the cross-linking to occur. The self-assembly of these block copolymers in water driven by the hydrophobic association of dithiolanes provides a high local concentration of dithiolanes in the core of micelles, which is essential for the thiol-initiated polymerization (cross-linking) to occur. These data also provide an explanation for the failure of the cross-linking reactions in organic solvents. In the absence of self-assembly, the concentrations of pendant dithiolanes groups on dissolved single chains are far below their $[M]_{eq}$ at room

DOI: 10.1021/jacs.7b00039
J. Am. Chem. Soc. 2017, 139, 3822−3833

temperature (in a 10 wt % solution, the concentration of dithiolane is only ~0.057 M), and thus no gelation was observed in organic solvents. This highlights the important role of both self-assembly and thiol-mediated oligomerization of dithiolanes in the dynamic gelation of these materials.

The mechanical strength and network stability of a dynamic covalent hydrogel are closely related to the thermodynamics (K_{eq}) of the reversible linkage.[12,24,25] The fraction of "active" disulfide cross-links in these hydrogels will be influenced by the K_{eq} of the ring-opening cascade of dithiolanes. The fact that K_{eq} of ROP of the lipoic acid-derived dithiolane **B** is approximately 3.2 times higher than that of the methyl asparagusic acid-derived dithiolane **A** suggests that more dithiolanes in the TMCLA-derived hydrogels are ring-opened to form active cross-links. This can be correlated to the higher G' and thus the higher stiffness and stability of the gels derived from the lipoic acid-derived hydrogels **5**/ODT as compared to that of the methyl asparagusic acid-derived hydrogel **2**/ODT (assuming that their physical cross-linking densities are not very different, as evidenced by the similar properties of the non-cross-linked physical gels). Because the K_{eq} of ring-opening polymerization of dithiolanes decreases with temperature, the amount of disulfide cross-links should decrease with increasing temperature. This explains the significant decrease in G' of **2**/ODT with increasing temperature and the gel−sol transition at around 42 °C. In contrast, the hydrogel derived from **5**/ODT showed only a small decrease in G' with temperature and no gel−sol transition. This is likely due to both the higher K_{eq} for ring-opening of lipoic acid and the slower rate of depolymerization, such that the gels derived from TMCLA **5** retain a sufficient number of cross-linked oligo(dithiolanes) that cannot depolymerize at a rate necessary to induce significant de-cross-linking at the given rate of heating (2 °C/min) (Figure 2D).

The lifetime (kinetics) of ring-opening and closing of dithiolanes is a key parameter for the dynamic and viscoelastic properties of these hydrogels.[25,76] The rate of gelation and self-healing should correspond closely with the rate of ring-opening (k_p), while the gel relaxation and adaption rate is related to the rate of ring-closure (k_d).[76] The slower exchange rates of dithiolane **B** accounts for the poorer recovery behavior of TMCLA gels as compared to TMCDT gels. The large differences in the flow behavior and stress relaxation rate between hydrogels derived from **5**/ODT and **2**/ODT can be attributed to the 14-fold difference in the depolymerization rate of dithiolanes: the lipoate dithiolane **B** has a much slower k_d than the methyl asparagusic acid dithiolane **A**, which contributes to the lack of flow and the slower stress relaxation rates of lipoate-derived gels **5**/ODT. It should be noted that in addition to thiol−disulfide exchange, the reversible formation of intermicellar bridges (physical cross-linking) also contributes to the dynamics and relaxation of these micellar gels.[12] The thermodynamics and time scale of these noncovalent linkages might be very different from those of the thiol−disulfide exchange but are rather similar between the two dithiolane-derived gels, as indicated by the similar properties of their physical gels. Therefore, the different properties of these gels are mainly caused by the differences in their chemical cross-linking. The two chain relaxation pathways, the chain-end pullout from micelles and the depolymerization of polydisulfides, are not independent as those dithiolanes that have ring-opened need to be released from the polydisulfide linkage for the polymer chain to detach from the micelle and re-enter another micelle, which makes a quantitative description of the viscoelastic property and relaxation behavior difficult. Nevertheless, the comparison of the thermodynamics and kinetics of the thiol−disulfide exchange provides a qualitative explanation for the structure−property relationship of these dithiolane-derived hydrogels.

CONCLUSION

The synthesis, self-assembly, and gelation behavior of a class of dithiolane-functionalized triblock copolymers composed of central poly(ethylene oxide) block and terminal polycarbonate blocks are described. These block copolymers were synthesized through expedient organocatalytic ring-opening polymerizations with precisely controlled molecular weights and narrow polydispersities. Self-assembly of these amphiphilic polymers in water forms flower-like micelles with dithiolane-rich cores. These flower micelles are physically cross-linked at high concentration to form a transient network to which the addition of a thiol triggers the chemical cross-linking of the core of the micelles through rapid and reversible ring-opening polymerizations of dithiolanes. Depending on the structure of the dithiolane, the resulting hydrogel can behave as a dynamic and adaptable network or a rigid and permanent network. The moduli, stress relaxation rate, and degradation profile of these dithiolane-derived hydrogels can be systematically tuned by varying the ratio of the two dithiolanes components through a copolymerization strategy. A detailed characterization of the thermodynamics and kinetics of ring-opening polymerization of different dithiolane monomers provides important insights on the structure−property relationship of these hydrogels: the dithiolane ring that has a lower tendency to ring-open, and faster rates of ring-opening and ring-closing constitute a significantly more dynamic and labile network. This study illustrates that the versatile chemistry of 1,2-dithiolanes can be utilized for constructing dynamic and responsive materials and that subtle differences in the rates and equilibria of thiol−disulfide exchange of 1,2-dithiolanes can lead to significant differences in the bulk material properties. We anticipate that the versatile behavior of dithiolanes will find use in a variety of contexts where reversible and environmentally responsive behavior is critical.

ASSOCIATED CONTENT

Supporting Information

The Supporting Information is available free of charge on the ACS Publications website at DOI: 10.1021/jacs.7b00039.

Experimental methods, synthetic methods and characterization of previously unreported compounds, as well as spectral and rheological data and GPC traces (PDF)

AUTHOR INFORMATION

Corresponding Author

*waymouth@stanford.edu

ORCID

Xiangyi Zhang: 0000-0003-4290-1600

Robert M. Waymouth: 0000-0001-9862-9509

Notes

The authors declare no competing financial interest.

ACKNOWLEDGMENTS

This material is based on work supported by the National Science Foundation (GOALI CHE-1607092) and the Office of

DOI: 10.1021/jacs.7b00039
J. Am. Chem. Soc. 2017, 139, 3822−3833

Naval Research (ONR-N00014-14-1-0551). X.Z. acknowledges a Stanford Graduate Fellowship and a LAM Graduate Fellowship.

REFERENCES

(1) Lutz, J. F.; Lehn, J. M.; Meijer, E. W.; Matyjaszewski, K. *Nat. Rev. Mater.* **2016**, *1*, 16024.
(2) Vougioukalakis, G. C.; Grubbs, R. H. *Chem. Rev.* **2010**, *110*, 1746−1787.
(3) Hawker, C. J.; Wooley, K. L. *Science* **2005**, *309*, 1200−1205.
(4) Ouchi, M.; Terashima, T.; Sawamoto, M. *Chem. Rev.* **2009**, *109*, 4963−5050.
(5) Kamber, N. E.; Jeong, W.; Waymouth, R. M.; Pratt, R. C.; Lohmeijer, B. G. G.; Hedrick, J. L. *Chem. Rev.* **2007**, *107*, 5813−5840.
(6) Zhou, C.; Toombes, G. E. S.; Wasbrough, M. J.; Hillmyer, M. A.; Lodge, T. P. *Macromolecules* **2015**, *48*, 5934−5943.
(7) Lee, A. L. Z.; Ng, V. W. L.; Gao, S. J.; Hedrick, J. L.; Yang, Y. Y. *Adv. Funct. Mater.* **2014**, *24*, 1538−1550.
(8) Cambon, A.; Figueroa-Ochoa, E.; Blanco, M.; Barbosa, S.; Soltero, J. F. A.; Taboada, P.; Mosquera, V. *RSC Adv.* **2014**, *4*, 60484−60496.
(9) Taribagil, R. R.; Hillmyer, M. A.; Lodge, T. P. *Macromolecules* **2010**, *43*, 5396−5404.
(10) Tsitsilianis, C. *Soft Matter* **2010**, *6*, 2372−2388.
(11) Balsara, N. P.; Tirrell, M.; Lodge, T. P. *Macromolecules* **1991**, *24*, 1975−1986.
(12) Winnik, M. A.; Yekta, A. *Curr. Opin. Colloid Interface Sci.* **1997**, *2*, 424−436.
(13) Rowan, S. J.; Cantrill, S. J.; Cousins, G. R. L.; Sanders, J. K. M.; Stoddart, J. F. *Angew. Chem., Int. Ed.* **2002**, *41*, 898−952.
(14) Lehn, J. M. *Chem. Soc. Rev.* **2007**, *36*, 151−160.
(15) Gasparini, G.; Dal Molin, M.; Lovato, A.; Prins, L. J. *Supramolecular Chemistry*; John Wiley & Sons, Ltd.: New York, 2012.
(16) Wojtecki, R. J.; Meador, M. A.; Rowan, S. J. *Nat. Mater.* **2011**, *10*, 14−27.
(17) Yang, Y.; Ding, X.; Urban, M. W. *Prog. Polym. Sci.* **2015**, *49*−*50*, 34−59.
(18) Li, C. H.; Wang, C.; Keplinger, C.; Zuo, J. L.; Jin, L.; Sun, Y.; Zheng, P.; Cao, Y.; Lissel, F.; Linder, C.; You, X. Z.; Bao, Z. A. *Nat. Chem.* **2016**, *8*, 619−625.
(19) Mukherjee, S.; Hill, M. R.; Sumerlin, B. S. *Soft Matter* **2015**, *11*, 6152−6161.
(20) Roy, N.; Bruchmann, B.; Lehn, J.-M. *Chem. Soc. Rev.* **2015**, *44*, 3786−3807.
(21) Barcan, G. A.; Zhang, X. Y.; Waymouth, R. M. *J. Am. Chem. Soc.* **2015**, *137*, 5650−5653.
(22) Michal, B. T.; Jaye, C. A.; Spencer, E. J.; Rowan, S. J. *ACS Macro Lett.* **2013**, *2*, 694−699.
(23) Wilson, A.; Gasparini, G.; Matile, S. *Chem. Soc. Rev.* **2014**, *43*, 1948−1962.
(24) Kloxin, C. J.; Bowman, C. N. *Chem. Soc. Rev.* **2013**, *42*, 7161−7173.
(25) Wang, H. Y.; Heilshorn, S. C. *Adv. Mater.* **2015**, *27*, 3717−3736.
(26) Wei, Z.; Yang, J. H.; Zhou, J. X.; Xu, F.; Zrinyi, M.; Dussault, P. H.; Osada, Y.; Chen, Y. M. *Chem. Soc. Rev.* **2014**, *43*, 8114−8131.
(27) Gantar, A.; Drnovsek, N.; Casuso, P.; Perez-San Vicente, A.; Rodriguez, J.; Dupin, D.; Novak, S.; Loinaz, I. *RSC Adv.* **2016**, *6*, 69156−69166.
(28) Casuso, P.; Odriozola, I.; Pérez-San Vicente, A.; Loinaz, I.; Cabañero, G.; Grande, H.-J.; Dupin, D. *Biomacromolecules* **2015**, *16*, 3552−3561.
(29) Holub, J.; Vantomme, G.; Lehn, J. M. *J. Am. Chem. Soc.* **2016**, *138*, 11783−11791.
(30) Canadell, J.; Goossens, H.; Klumperman, B. *Macromolecules* **2011**, *44*, 2536−2541.
(31) Lafont, U.; van Zeijl, H.; van der Zwaag, S. *ACS Appl. Mater. Interfaces* **2012**, *4*, 6280−6288.
(32) Fairbanks, B. D.; Singh, S. P.; Bowman, C. N.; Anseth, K. S. *Macromolecules* **2011**, *44*, 2444−2450.
(33) Otsuka, H.; Nagano, S.; Kobashi, Y.; Maeda, T.; Takahara, A. *Chem. Commun.* **2010**, *46*, 1150−1152.
(34) Wiita, A. P.; Ainavarapu, R. K.; Huang, H. H.; Fernandez, J. M. *Proc. Natl. Acad. Sci. U. S. A.* **2006**, *103*, 7222−7227.
(35) Black, S. P.; Sanders, J. K. M.; Stefankiewicz, A. R. *Chem. Soc. Rev.* **2014**, *43*, 1861−1872.
(36) Pepels, M.; Filot, I.; Klumperman, B.; Goossens, H. *Polym. Chem.* **2013**, *4*, 4955−4965.
(37) Yoon, J. A.; Kamada, J.; Koynov, K.; Mohin, J.; Nicolay, R.; Zhang, Y. Z.; Balazs, A. C.; Kowalewski, T.; Matyjaszewski, K. *Macromolecules* **2012**, *45*, 142−149.
(38) Gyarmati, B.; Nemethy, A.; Szilagyi, A. *Eur. Polym. J.* **2013**, *49*, 1268−1286.
(39) Endo, K.; Shiroi, T.; Murata, N.; Kojima, G.; Yamanaka, T. *Macromolecules* **2004**, *37*, 3143−3150.
(40) Kisanuki, A.; Kimpara, Y.; Oikado, Y.; Kado, N.; Matsumoto, M.; Endo, K. *J. Polym. Sci., Part A: Polym. Chem.* **2010**, *48*, 5247−5253.
(41) Bang, E. K.; Lista, M.; Sforazzini, G.; Sakai, N.; Matile, S. *Chem. Sci.* **2012**, *3*, 1752−1763.
(42) Sadownik, A.; Stefely, J.; Regen, S. L. *J. Am. Chem. Soc.* **1986**, *108*, 7789−7791.
(43) Li, Y. L.; Zhu, L.; Liu, Z.; Cheng, R.; Meng, F.; Cui, J. H.; Ji, S. J.; Zhong, Z. *Angew. Chem., Int. Ed.* **2009**, *48*, 9914−9918.
(44) Drake, C. R.; Aissaoui, A.; Argyros, O.; Serginson, J. M.; Monnery, B. D.; Thanou, M.; Steinke, J. H. G.; Miller, A. D. *Mol. Pharmaceutics* **2010**, *7*, 2040−2055.
(45) Balakirev, M.; Schoehn, G.; Chroboczek, J. *Chem. Biol.* **2000**, *7*, 813−819.
(46) Wei, R. R.; Cheng, L.; Zheng, M.; Cheng, R.; Meng, F. H.; Deng, C.; Zhong, Z. Y. *Biomacromolecules* **2012**, *13*, 2429−2438.
(47) Yang, W. J.; Zou, Y.; Meng, F. H.; Zhang, J.; Cheng, R.; Deng, C.; Zhong, Z. Y. *Adv. Mater.* **2016**, *28*, 8234−8239.
(48) Zhong, Y. N.; Zhang, J.; Cheng, R.; Deng, C.; Meng, F. H.; Xie, F.; Zhong, Z. Y. *J. Controlled Release* **2015**, *205*, 144−154.
(49) Zou, Y.; Meng, F. H.; Deng, C.; Zhong, Z. Y. *J. Controlled Release* **2016**, *239*, 149−158.
(50) Zou, Y.; Fang, Y.; Meng, H.; Meng, F.; Deng, C.; Zhang, J.; Zhong, Z. *J. Controlled Release* **2016**, *244*, 326−335.
(51) Zhang, N.; Xia, Y.; Zou, Y.; Yang, W.; Zhang, J.; Zhong, Z.; Meng, F. *Mol. Pharmaceutics* **2017**, ASAP, DOI: 10.1021/acs.molpharmaceut.6b00800.
(52) Sakai, N.; Lista, M.; Kel, O.; Sakurai, S.; Emery, D.; Mareda, J.; Vauthey, E.; Matile, S. *J. Am. Chem. Soc.* **2011**, *133*, 15224−15227.
(53) Sakai, N.; Matile, S. *J. Am. Chem. Soc.* **2011**, *133*, 18542−18545.
(54) Bang, E. K.; Gasparini, G.; Molinard, G.; Roux, A.; Sakai, N.; Matile, S. *J. Am. Chem. Soc.* **2013**, *135*, 2088−2091.
(55) Gasparini, G.; Bang, E. K.; Molinard, G.; Tulumello, D. V.; Ward, S.; Kelley, S. O.; Roux, A.; Sakai, N.; Matile, S. *J. Am. Chem. Soc.* **2014**, *136*, 6069−6074.
(56) Houk, J.; Whitesides, G. M. *J. Am. Chem. Soc.* **1987**, *109*, 6825−6836.
(57) Lees, W. J.; Whitesides, G. M. *J. Org. Chem.* **1993**, *58*, 642−647.
(58) Singh, R.; Whitesides, G. M. *J. Am. Chem. Soc.* **1990**, *112*, 6304−6309.
(59) Singh, R.; Whitesides, G. M. *J. Am. Chem. Soc.* **1990**, *112*, 1190−1197.
(60) *Creep and Relaxation of Nonlinear Viscoelastic Materials with an Introduction to Linear Viscoelasticity*; Findley, W. N., Lai, J. S., Onaran, K., Eds.; Dover: New York, 1989.
(61) Hocine, S.; Li, M. H. *Soft Matter* **2013**, *9*, 5839−5861.
(62) Ward, M. A.; Georgiou, T. K. *Polymers* **2011**, *3*, 1215−1242.
(63) Mortensen, K.; Brown, W.; Jorgensen, E. *Macromolecules* **1994**, *27*, 5654−5666.
(64) Kalyanasundaram, K.; Thomas, J. K. *J. Am. Chem. Soc.* **1977**, *99*, 2039−2044.
(65) Vagberg, L. J. M.; Cogan, K. A.; Gast, A. P. *Macromolecules* **1991**, *24*, 1670−1677.

DOI: 10.1021/jacs.7b00039
J. Am. Chem. Soc. 2017, 139, 3822−3833

(66) Voorhaar, L.; De Meyer, B.; Du Prez, F.; Hoogenboom, R. *Macromol. Rapid Commun.* **2016**, *37*, 1682−1688.
(67) Morelli, P.; Martin-Benlloch, X.; Tessier, R.; Waser, J.; Sakai, N.; Matile, S. *Polym. Chem.* **2016**, *7*, 3465−3470.
(68) Page, S. M.; Martorella, M.; Parelkar, S.; Kosif, I.; Emrick, T. *Mol. Pharmaceutics* **2013**, *10*, 2684−2692.
(69) Koo, A. N.; Lee, H. J.; Kim, S. E.; Chang, J. H.; Park, C.; Kim, C.; Park, J. H.; Lee, S. C. *Chem. Commun.* **2008**, 6570−6572.
(70) Ryu, J. H.; Roy, R.; Ventura, J.; Thayumanavan, S. *Langmuir* **2010**, *26*, 7086−7092.
(71) Vandeputte, A. G.; Sabbe, M. K.; Reyniers, M.-F.; Marin, G. B. *Chem. - Eur. J.* **2011**, *17*, 7656−7673.
(72) Bach, R. D.; Dmitrenko, O.; Thorpe, C. *J. Org. Chem.* **2008**, *73*, 12−21.
(73) Gasparini, G.; Sargsyan, G.; Bang, E. K.; Sakai, N.; Matile, S. *Angew. Chem., Int. Ed.* **2015**, *54*, 7328−7331.
(74) Dubois, P.; Coulembier, O.; Raquez, J.-M. *Handbook of Ring-Opening Polymerization*; Wiley-VCH: Weinheim, 2009.
(75) Odian, G. *Principles of Polymerization*, 4th ed.; Wiley-Interscience: New York, 2004.
(76) McKinnon, D. D.; Domaille, D. W.; Cha, J. N.; Anseth, K. S. *Chem. Mater.* **2014**, *26*, 2382−2387.

DOI: 10.1021/jacs.7b00039
J. Am. Chem. Soc. 2017, 139, 3822−3833